EFFECTS OF THERMAL LOADING ON NON-LINEAR IN-PLANE BUCKLING OF SHALLOW CROWN-PINNED STEEL ARCHES

Y.-L. PI[1*], M.A. BRADFORD[1], Y.-L. GUO[2], C. DOU[2]

[1]*Centre of Infrastructure Engineering and Safety, School of Civil and Environmental Engineering, The University of New South Wales, Australia*

[2]*School of Civil Engineering, Tsinghua University, China*

ABSTRACT

This paper investigates the effects of thermal loading on the non-linear in-plane elastic buckling of shallow crown-pinned circular steel arches that is subjected to a uniform radial load. Differential equations of equilibrium are derived based on the principle of virtual work, and analytic solutions for the non-linear buckling loads are obtained. It is found that the thermal loading influences the non-linear buckling of shallow crown-pinned steel arches significantly. The non-linear buckling loads increases with an increase of the temperature. It is also founded that crown-pinned arches can buckle in a limit point instability mode, but cannot buckle in a bifurcation mode.

Keywords: Buckling, crown-pinned arches, thermal loading, limit point instability.

1. INTRODUCTION

In many cases arches are built by joining two separate curvilinear segments together at the crown, thereby reducing the arch size to meet transport requirements and to create a statically determinate structure when the arch is also pin-ended which is insensitive to detrimental effects of foundation settlements.

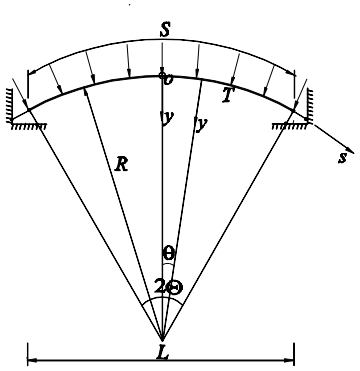

Figure 1: Crown-pinned circular arch.

The joint location is often significantly weaker compared to the arch-rib, and so can be idealized as a pin.

* Corresponding author: Email: y.pi@unsw.edu.au

This crown pin is able to transfer shear forces and normal forces but is unable to resist bending moments, leading to free rotation of the arch segments about the pin. This will affect the structural response of the arch to loading. When a shallow crown-pinned steel arch is subjected to thermal loading produced by a temperature increase, the thermal loading produces the additional deformations of the arch. Because of the nonlinearity of shallow arches, the thermal deformations will interact with the non-linear deformations produced by the uniform radial load and these may influence the non-linear equilibrium of the arch and its buckling and postbuckling behaviour (Pi and Bradford 2010a, 2010b). This paper presents an investigation of the influence of the thermal loading on the non-linear in-plane elastic buckling of crown-pinned circular steel arches with pinned (three-pinned arches) or fixed ends (one-pinned arches) (Figure 1). Differential equations of equilibrium are derived based on the principle of virtual work, and analytical solutions for the elastic buckling loads are derived.

2. NON-LINEAR EQUILIBRIUM

Because the effect of the crown-pin has to be considered, the half arch shown in Figure 1 is used to derive the differential equations of equilibrium by using the principle of virtual work, which states that

$$\delta\Pi = \int_0^{\Theta} [-NR(\delta\tilde{w}' - \delta\tilde{v} + \tilde{v}'\delta\tilde{v}') - M\delta\tilde{v}'' - qR^2]\mathrm{d}\theta = 0, \tag{1}$$

where Θ is the half included angle of the arch (Figure 1), N and M are the axial compressive force and bending moment and from the Duhamel-Neumann equation (1978 Nowinski) they can be expressed as

$$N = AE_T[\alpha\Delta T - (\tilde{w}' - \tilde{v} + \frac{1}{2}\tilde{v}'^2)] \quad \text{and} \quad M = -E_T I_x \frac{\tilde{v}''}{R}, \tag{2}$$

in which the temperature increase $\Delta T = T - T_0$, T is the temperature, T_0 is the temperature of the arch in the normal service condition, A and I_x are the area and the second moment of area of the cross-section, R is the initial radius of the arch, and E_T is the temperature-dependent modulus of elasticity of the steel. The expression of E_T proposed in Australian design code for steel structures AS4100 is used in this paper, which is written as (Pi and Bradford 2010c)

$$E_T = E_{20}\left[1 + \frac{T}{2000\ln(T/110)}\right] \quad \text{for} \quad 0^\circ C < T \le 600^\circ C. \tag{3}$$

Integrating equation (1) by parts leads to differential equations of equilibrium as

$$N' = 0 \quad \text{and} \quad \frac{\tilde{v}^{iv}}{\mu^2} + \tilde{v}'' = P \quad \text{with} \quad \mu^2 = \frac{NR^2}{EI_x} \quad \text{and} \quad P = \frac{qR - N}{N}, \tag{4}$$

and leads to the static boundary conditions

$$\tilde{v}'' = 0 \quad \text{and} \quad \frac{EI_x \tilde{v}'''}{R} + NR\tilde{v}' = 0 \quad \text{at } \theta = 0 \tag{5}$$

for one and three-pinned arches, and

$$\tilde{v}'' = 0 \quad \text{at} \quad \theta = \Theta \tag{6}$$

for three-pinned arches.

In addition, the essential kinematical boundary conditions for one and three-pinned arches are

$$\tilde{w} = 0 \quad \text{at} \quad \theta = 0 \quad \text{and} \quad \theta = \Theta, \text{ and } \tilde{v} = 0 \quad \text{at} \quad \theta = \Theta. \tag{7}$$

The dimensionless radial displacement can be obtained by solving equation (4) under the boundary conditions given by equations (5)-(7) as

$$\tilde{v} = \frac{P}{\mu^2}\left[\cos\mu\theta - 1 + + \frac{H(\theta)(1-\cos\beta)\sin\mu\theta}{\sin\beta} + \frac{1}{2}(\mu^2\theta^2 - \beta^2)\right] \tag{8}$$

for three-pinned arches, and

$$\tilde{v} = \frac{P}{\mu^2}\left(\cos\mu\theta - \frac{1}{\cos\beta} + H\tan\beta\sin\mu\theta\right) + \frac{P}{\mu^2}\left[\beta\tan\beta + \frac{1}{2}(\mu^2\theta^2 - \beta^2) - \frac{H\beta\sin\mu\theta}{\cos\beta}\right] \tag{9}$$

for one-pinned arches, where the dimensionless axial force parameter $\beta = \mu\Theta$ and the step function $H(\theta)$ is defined as

$$H(\theta) = \begin{cases} -1 & \text{when} \quad \theta < 0 \\ 1 & \text{when} \quad \theta \geq 0 \end{cases} \tag{10}$$

From the first of equation (4), the axial compressive force is a constant. Substituting the solutions given by equations (8) and (9) into the first of equation (2) and integrating over the arch length lead to the equations between the dimensionless load P and the dimensionless axial compressive force parameter β as

$$A_1 P^2 + A_2 P + A_3 = 0 \tag{11}$$

where the coefficients A_1, A_2, and A_3 are given by

$$A_{11} = \frac{1}{\beta^2}\left[1 - \frac{5\sin\beta - \beta}{2\beta(1+\cos\beta)}\right] + \frac{1}{6}, \quad A_{21} = \frac{1}{\beta^2}\left[1 - \frac{2\sin\beta}{\beta(1+\cos\beta)}\right] + \frac{1}{3}, \tag{12}$$

$$A_3 = \frac{\beta^2}{\lambda^2} - \frac{\alpha\Delta T}{\Theta^2}, \quad \lambda = \frac{\Theta S}{2r_x} \tag{13}$$

for three-pinned arches, and

$$A_1 = \frac{1}{4\beta^2}\left[\frac{8}{\cos\beta} + (1+\beta^2)\sec^2\beta - \frac{5\tan\beta}{\beta} - 4\right] - \frac{\tan\beta}{2\beta}\left(\frac{3}{2} + \frac{1}{\cos\beta}\right) + \frac{1}{6}, \tag{14}$$

$$A_2 = \frac{1}{\beta^2}\left(\frac{2}{\cos\beta} - 1\right) - \frac{\tan\beta}{\beta}\left(1 + \frac{1}{\beta^2}\right) + \frac{1}{3}, \quad A_3 = \frac{\beta^2}{\lambda^2} - \frac{\alpha\Delta T}{\Theta^2}, \quad \lambda = \frac{\Theta S}{2r_x} \tag{15}$$

for one-pinned archers.

The non-linear equilibrium paths and the effects of the temperature change are shown in Figures 2 for a three-pinned steel arch as variations of the dimensionless load qR/N_E with the dimensionless central radial displacement v_c/f, where the thermal expansion coefficient of steel $\alpha = 11.3 \times 10^{-6}$ is adopted, and N_E is the second mode flexural buckling load of a corresponding pin-ended column under uniform axial compression and given by

$$N_E = \frac{E_T I_x \pi^2}{(S/2)^2} \tag{16}$$

in which S is the length of the arch.

It can be seen from Figures 2 that when the upper limit point is reached, further increase of the displacement is associated with a decrease of the external load and with a decrease of the axial force along the unstable path until the lower limit point is reached. Following this, as the displacement continues to increase, the external load increases again along the remote stable equilibrium path (Figures 2(a) and 2(b)), but the axial compressive force continues to decrease until vanishes and then the axial force changes to tension (Figures 2(c) and 2(d)).

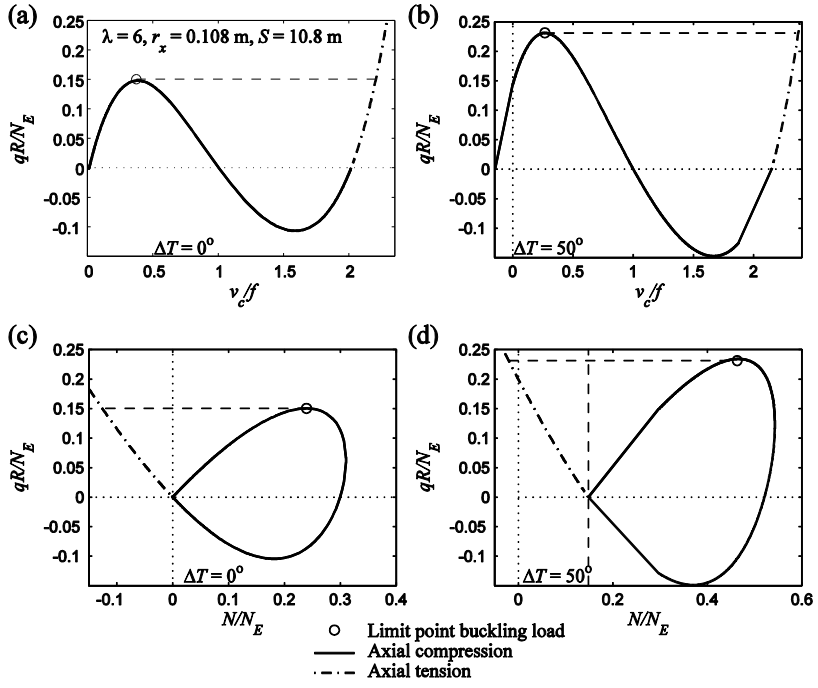

Figure 2: Non-linear equilibrium paths of a three-pinned arch.

By comparing Figure 2(a) (or Figure 2(c)) with Figure 2(b) (or Figure 2(d)), it can be seen that the arch under a uniform temperature field ΔT = 50°C has an initial upward radial displacement (i.e. in the convex direction of the arch) (Figure 2(b)) and an initial axial compressive force (Figure 2(d))

while it has no initial radial displacement and axial compressive force when ΔT = 0°C (Figures 2(a) and 2(c)). The upper limit buckling loads of the arch when ΔT = 50°C (Figures 2(b) and 2(d)) are higher than those when ΔT = 0°C (Figures 2(a) and (2c)). It is noted when the axial force changes from compression to tension, the value of μ defined in equation (4) and the value of $\beta=\mu\Theta$ becomes imaginary numbers. In this case, the trigonometric functions in expressions for the radial displacement (equations (8) and (9)) and for the coefficients of equation (11) have to be converted to the corresponding hyperbolic functions by performing the following operations: $\mu \to i\mu$, $\beta \to i\beta$, $\sin(i\beta) = i\sinh(\beta)$, $\cos(i\beta) = \cosh(\beta)$, and $\tan(i\beta) = i\tanh(\beta)$. The imaginary unit i will be cancelled out.

The non-linear equilibrium paths of one-pinned arches are somewhat different from that of three-pinned arches as shown in Figures 3. Because both ends are fixed, the buckling load of the one-pinned arches is higher than that of the three-pinned arch. However, the effects of temperature changes on the structural responses of one-pinned arches are similar to those on three-pinned arches. It can be seen again that arch under a uniform temperature field ΔT = 80°C has an initial upward radial displacement (Figure 3(b)) and an initial axial compressive force (Figure 3(d)) and that The upper limit buckling loads of the arch when ΔT = 80°C (Figures 3(b) and 3(d)) are higher than those when ΔT = 0°C (Figures 3(a) and (3c)).

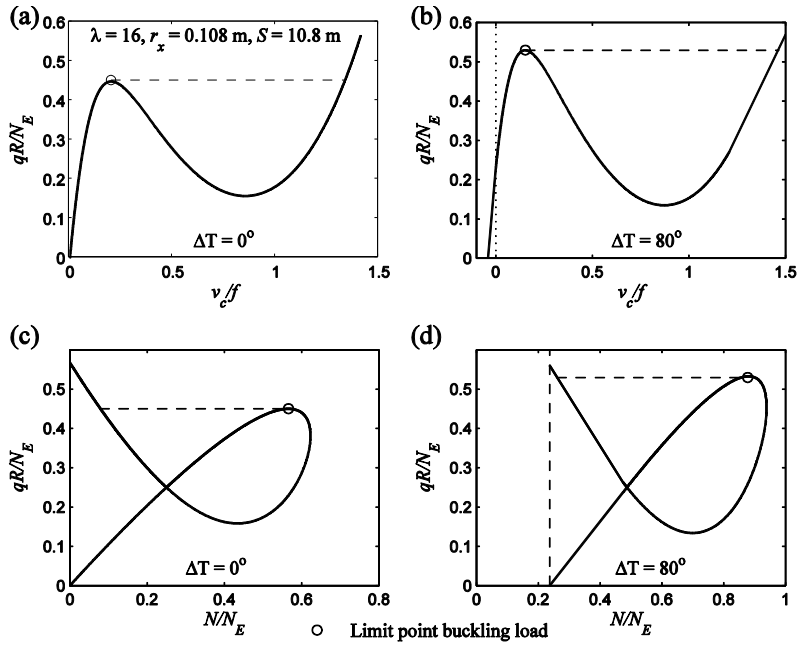

Figure 3: Non-linear equilibrium paths of a one-pinned arch.

3. LIMIT POINT INSTABILITYAND BIFURCATION BUCKLING

Because the limit points are local extrema on the non-linear equilibrium paths, so differentiating equation (11) with respect to β leads to the equilibrium equation between the dimensionless load P and the axial force parameter β at the limit points as

$$B_1 P^2 + B_2 P + B_3 = 0 \tag{17}$$

where the coefficients B_1, B_2, and B_3 are given by

$$B_1 = 2A_1 - \frac{\beta \partial A_1}{2\partial \beta}, \quad B_2 = 4A_1, \quad B_3 = A_2 - \frac{\beta^2}{\lambda^2}. \tag{18}$$

Solving equations (11) and (17) simultaneously leads to the limit point buckling load and the corresponding axial force as shown in Figures 2 and 3.

In addition to limit point instability, possibility of bifurcation buckling of crown-pinned steel arches is herein investigated. It has been shown (Pi et al. 2002) that the shape of bifurcation buckling is antisymmetric and that during bifurcation buckling, the nominal axial force qR is equal to the second mode flexural buckling load of a pin-ended column under uniform axial compression N_E given by equation (16). However, the value of qR in a crown-pinned steel arch for the symmetric limit buckling loads are lower than N_E as shown in Figure 4. Therefore, crown-pinned steel arches can buckle in a symmetric limit point instability mode under a load lower than N_E, but cannot buckle in an antisymmetric bifurcation mode. It can also be seen from Figure 4 that as the modified slenderness of the arch λ decreases, the effects of thermal expansion on the in-plane buckling of crown-pinned steel aches increases.

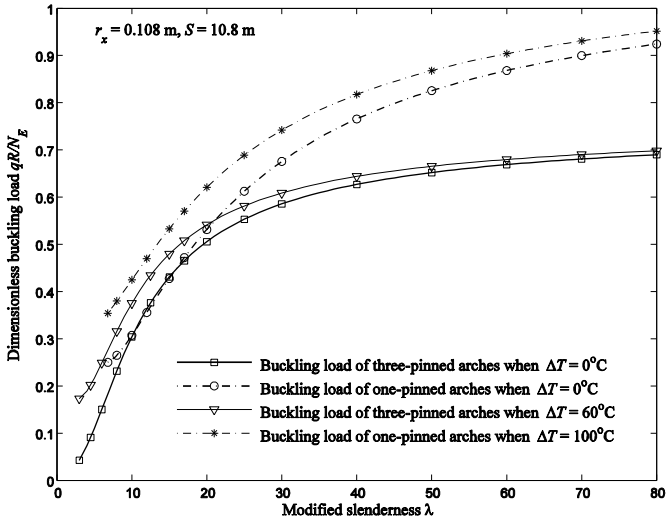

Figure 4: Buckling loads.

4. CONCLUSIONS

Effects of thermal loading on the non-linear in-plane elastic buckling of shallow crown-pinned circular steel arches under a uniform radial load have been investigated. It has been shown that the thermal loading influences the non-linear buckling of shallow crown-pinned steel arches significantly. The non-linear buckling loads increases with an increase of the temperature. It was also shown that the crown-pinned arches can buckle in a limit point instability mode, but cannot buckle in a bifurcation mode.

ACKNOWLEDGMENTS

This work has been supported by the Australian Research Council through Discovery Projects (DP1097096 and DP1096454) by awarded to both authors and an Australian Laureate Fellowship (FL100100063) awarded to the second author.

REFERENCES

Nowinski JL (1978). Theory of thermoelasticity with applications. Alphen aan den Rijn, The Netherlands: Sijthoff & Noordhoff International Publishers.

Pi Y-L and Bradford MA (2010a). Nonlinear in-plane elastic buckling of shallow circular arches under uniform radial and thermal loading. International Journal of Mechanical Sciences 52, pp. 75-88.

Pi Y-L and Bradford MA (2010b). Non-linear thermoelastic buckling of pin-ended arches under temperature gradient. Journal of Engineering Mechanics ASCE 136(8), pp. 960-968.

Pi Y-L and Bradford MA (2010c). In-plane thermoelastic behaviour and buckling of pin-ended and fixed circular arches. Engineering Structures 32(1), pp.250-260.

Pi Y-L, Bradford MA, and Uy B. (2002). In-plane stability of arches. International Journal of Solids and Structures. 39, pp.105-125.